American Mineralogist, Volume 70, pages 1169–1179, 1985

The high temperature behavior of trace hydrous components in silicate minerals

ROGER D. AINES[1] AND GEORGE R ROSSMAN

Division of Geological and Planetary Sciences[2]
California Institute of Technology
Pasadena, California 91125

Abstract

We have studied the high temperature behavior of water and hydroxide in quartz, feldspar, topaz, zircon, muscovite, cordierite, and beryl using high temperature infrared spectroscopy. We have directly observed processes such as dehydration and changes in hydrogen speciation. In some minerals trace hydroxyl and water speciation and properties at temperatures of geologic interest can be dramatically different from those at 25°C. In muscovite, no changes in speciation occur prior to dehydration at 750°C, whereas in topaz hydroxyl sites interconvert at 500°C. In metamict zircon strongly hydrogen-bonded hydroxyl is preferentially lost from a continuum of sites during continuous dehydration occurring from 400° to 900°C. There are only minor changes in the O–H region spectrum of natural quartz at the α–β transition point. In feldspar one type of molecular water is lost at ~200°C, and at 600° to 800° a second water type converts irreversibly to a new hydrous species. Changes at high temperature common to the infrared absorption bands of all minerals studied are: broadening, a shift to lower wavenumbers, and a slight decrease in integral intensity. Temperature coefficients for O–H stretching peak shifts range from 0 to -0.045 cm^{-1}/°C. Lattice modes also broaden and shift to lower wavenumbers, typically with temperature coefficients of about -0.03 cm^{-1}/°C.

Introduction

Studies of minerals and their properties usually utilize measurements near 25°C. This is experimentally convenient but may only provide a limited insight into the properties of minerals at the elevated temperatures typical of conditions of geologic interest. Trace "water" in silicates can have a substantial effect on the properties of minerals (e.g., Aines and Rossman, 1984a, 1985; Kekulawala et al., 1978; Hobbs, 1981), but because hydrous components in minerals are reactive and mobile, the high temperature speciation and sites of hydrous components may not be the same as those at room temperature. Accordingly, we have undertaken a study of trace hydrous components at elevated temperature in order to understand the types of behavior that may be expected of trace water under geologic conditions.

We have used high temperature infrared (IR) spectroscopy because of its sensitivity to O–H bonds, and because spectra may be obtained at elevated temperatures, allowing direct interpretation. This technique has been used previously to study the thermal conductivity of glasses (e.g., Wedding, 1975; Stein and Shankland, 1981) and minerals (Aronson et al., 1970; Shankland et al., 1979). Studies of hydrous components at elevated temperatures are limited to glasses (Wedding, 1975), $Mg(OH)_2$ (Freund, 1970, 1974), and other synthetics (Freund, 1974; Aines, 1984). We have previously reported on the high temperature behavior of water and carbon dioxide in cordierite and beryl (Aines and Rossman, 1984b) and will report additional aspects of that study here. Some theoretical aspects of peak shifts and shape changes caused by temperature change are discussed by Aines (1984).

We use the term trace water to refer to hydrous components of any unidentified species. The only hydrogen species in silicate minerals for which firm evidence exists are hydroxyl (OH^-) and molecular water (H_2O) (Aines and Rossman, 1984a) and atomic and molecular hydrogen which may be formed by intense radiolysis of minerals (see Aines, 1984, and references therein). Unfortunately, the last two species have no IR manifestation and are generally undetectable in IR studies. Other postulated hydrogen species in silicates are oxonium, H_3O^+ and silicon hydride groups, SiH.

Experimental method

High temperature apparatus

Spectra were obtained at high temperature by placing the sample in a small tube furnace, aligned in the direction of the spectrometer beam. The samples were mounted on stainless steel apertures which completely filled the cross-section of the furnace, allowing light only to pass through the sample. The furnace is contained in a vacuum dewar with KCl windows; this eliminates

[1] Present address: University of California, Lawrence Livermore National Laboratory, Earth Sciences Department, P.O. Box 808, Livermore, CA 94550.

[2] Contribution number: 4174.

0003–004X/85/1112–1169$02.00

heating of the spectrometer and also avoids oxidation of furnace parts. Details of the construction of each of these parts follow.

The furnace and sample assembly are shown schematically in Figure 1. The furnace tube is grooved to accept the windings of a Pt(80%)–Rh(20%) resistance wire designed to be operable to 1400°C. The furnace temperature is controlled via the sample thermocouple and a proportioning controller which provides stable control from ~300° to 1200°C. Below 300° the thermal mass of the furnace limits response time, and fluctuations of 10–15°C over 20 minutes can occur.

The vacuum container is constructed of welded 1/4″ aluminum with KCl windows. Liquid nitrogen traps are placed in the vacuum line to catch pump oil and volatiles evolved from the furnace.

The samples used are oriented, doubly polished single crystal slabs. These are mounted on circular stainless steel (type 303) apertures which are machined to allow maximum light passage through irregularly shaped samples. Typical apertures are 5 to 20 mm^2; apertures smaller than 5 mm^2 result in problems with the black body correction. The sample is held over the aperture by straps made of 25 μm stainless steel shim shock, spot welded onto the aperture disc.

The sample disc is held upright and centered in the furnace by two machinable ceramic rings which are easy press-fits into the furnace tube. An additional ceramic piece is used to mask off black body radiation from the stainless steel disk. This disc is placed in the end of the furnace tube through which light exits toward the detector. It has a conical hole in the center which is shaped to allow maximum light from the sample to pass through.

A minimum of two thermocouples are used in each run. One is permanently mounted on the inside of the furnace tube at the center position. The second is mounted on the sample disc, adjacent to the sample. Typical thermal gradients measured in this way across the radius of the furnace have not exceeded 10°C. When the sample is sufficiently thick, as for our quartz studies, an additional thermocouple may be mounted on the sample, in the beam path. This was accomplished by drilling a small hole in the center of the sample, and cementing a thermocouple into it directly in the center of the illuminated area. This yielded an average temperature for the section of the sample actually being observed, which was approximately 3 × 5 mm in cross section. The thermocouple mounted on the stainless steel aperture was as much as 2° hotter than the sample, and the rim of the sample aperture (at the wall of the furnace) registered up to 10° hotter than the sample.

Spectrophotometer

A Perkin-Elmer model 180 spectrophotometer is used to collect infrared spectra. Its optical and detector system make it uniquely suited to the task of high temperature spectroscopy. The beam passes through the sample and reference before being monochromatized by a diffraction grating thus minimizing the amount of black body radiation from the sample which strikes the detector. This avoids overloading the detector. The black body emission is electronically subtracted from the spectrophotometer beam by a double chopping system, which alternately measures the transmitted and emitted light. Accurate subtraction of the emission is easily obtainable up to 1200°C provided that the stainless steel aperture has been adequately masked off, and the detector "sees"

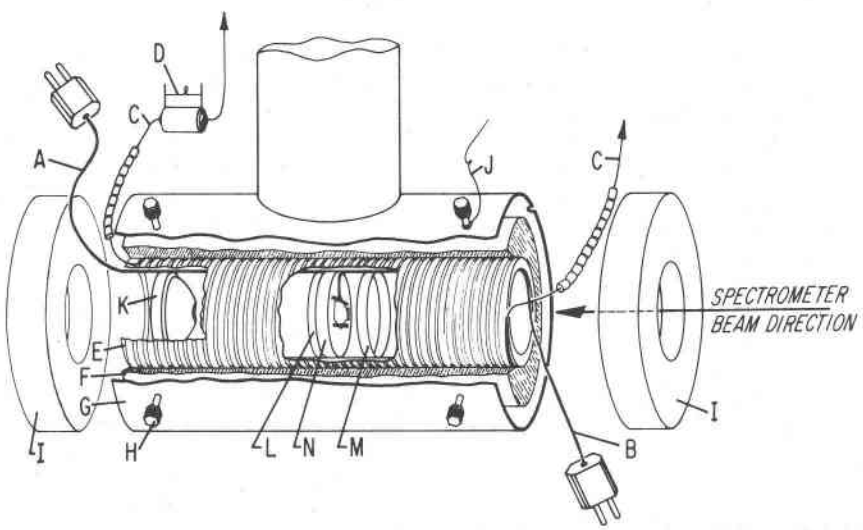

Fig. 1. Schematic diagram of the furnace and sample assembly. View is cut-away and partially exploded. This portion of the apparatus is contained within the vacuum dewar. (A) Permanent thermocouple, cemented to furnace wall at center point. (B) Sample thermocouple, welded to aperture next to sample or cemented to the sample. (C) Furnace winding. Alumina insulating beads are used to keep the bare wire from contacting the steel support structure. (D) Fuse made of furnace winding wire. (E) Mullite furnace tube. (F) Alumina insulating tube. Furnace tube is a press-fit into this. (G) Stainless steel support tube. This tube is suspended from the lid of the dewar by a second stainless steel tube (shown cut off here.) (H) Screws (radial to support tube) support and align the furnace. There is a 5 mm gap between the stainless steel support tube and the furnace insulation. (I) Alumina insulating discs to mask black body radiation from exterior of furnace. These are held in place by nichrome wire wrapped around the support screws. (J) Nichrome wire to hold discs. (K) Machinable alumina cone to mask unwanted black body radiation from interior of furnace, and stainless steel aperture. (L) Ceramic ring cemented in furnace center to align and support the sample. Permanent thermocouple is cemented between this ring and the furnace wall. (M) Movable ceramic ring, loose press fit to the furnace wall. This ring is inserted after the sample mount, and holds the sample mount snugly against the permanent ring. (N) Sample assembly. Sample is held on stainless steel aperture with stainless steel strips spotwelded in place; these also hold the sample thermocouple.

only limited emissions from the rest of the furnace. When black body emissions are too large, for instance if the furnace were run with no thermal baffles, the thermopile detector overloads resulting in an apparent phase-shift.

The furnace dewar is mounted in the sample compartment in an X–Y–Z translation stage to allow accurate positioning. Typical absolute transmission using this system is about 12%; the losses are largely due to window reflection, collimation of the focused beam by the furnace parts, and the restriction of the aperture. Quantitative results may be obtained down to about 0.01% absolute transmittance.

The spectrophotometer is interfaced to a DEC MINC-11 computer system which is used to collect both spectra and kinetics data (absorbance vs. time). This interface directly utilizes the PE-180 digital absorbance and frequency information, allowing quantitative measurements up to absorbances of 2. The spectra and data in this paper were checked against standard absorption screens and are accurate to within 2% of the stated absorbance value.

The most significant component in the spectral baseline of this system is due to organics which outgas from the furnace cements and insulation and condense on the cool KCl dewar windows. This results in several sharp C–H stretching bands near 2900 cm^{-1}. The baseline is checked frequently and subtracted by computer from the spectra. In practice, the windows require replacement infrequently, typically after about 30 hrs at 900°C.

The most significant problem in this system is caused by samples cracking under thermal stress or dehydration which limited our work in silicate crystals to 800–900°C.

Results and discussion

Muscovite

The hydroxyl in muscovite is not a "trace" hydrous component, but was included in this study in order to understand the type of behavior to be expected from a single, well defined hydroxyl site at high temperature. This is required to verify that the effects observed in other mineral systems are not spurious effects of temperature.

Figure 2 shows the reversible aspects of the changes in the O–H stretching band with temperature. The 40° peak shifts slightly at 590° and there is a slight decrease in integrated intensity. Upon cooling the original spectrum is once more obtained. (The "cooled" temperature in this run is 40°C because of heating by the spectrometer beam; this varies somewhat from sample to sample and depending on the type of thermal baffles in place.) No new O–H absorptions form during dehydration above 750°C. There is only a monotonic decrease in intensity of the original band.

The lack of new absorptions, and hence observable intermediate species, is in contrast to a 1970 study by Freund of the dehydration of $Mg(OH)_2$ (see also Freund, 1974). He observed just prior to dehydration a slight broadening of the O–H peak and interpreted this as evidence of proton tunneling between OH sites. This is one way to form H_2O molecules which are the observed dehydration species. There is no evidence of such a process in muscovite, and no reason to believe that H_2O molecules are not formed by simple diffusional hopping of H^+ to an adjacent OH^- site. These H_2O molecules would be free to rapidly diffuse out of the sample, which was thin at the outset of the experiment (11 μm), and exfoliated to ~ 2 μm sheets during dehydration.

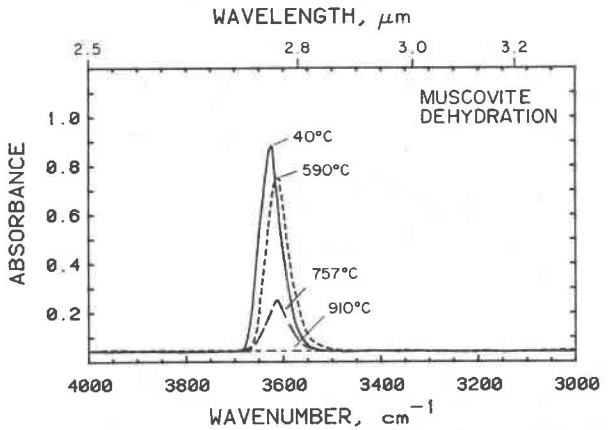

Fig. 2. Infrared spectra of an 11 μm thick cleavage flake of muscovite showing thermal effects on the O–H stretching absorption. Spectra obtained at the indicated temperatures. The slight broadening and frequency shift at 590° is completely reversible upon cooling. The 757° spectrum was obtained during active dehydration. The sample recovered after dehydration at 910° had exfoliated to a thickness of about 2 μm. Spectra obtained in the β polarization, E$\|a$, the minimum O–H intensity direction.

Cordierite and beryl

We have previously reported on changes in H_2O site and the dehydration mechanism of these minerals (Aines and Rossman, 1984b). Here we address the peak shifts in these minerals with temperature. The relationship between O–H–O distance and O–H stretching frequency may allow extraction of structural information from thermally induced peak shifts. For hydrogen-bonded systems, several different mechanisms should result in positive peak shifts; systems in which hydrogen bonding is unimportant should have negative peak shifts (Aines, 1984). In both cases this is due to the average increase in O–O, and hence O–H–O, distance with temperature. In hydrogen-bonded systems it has been suggested that as O–H–O distance increases, so should the absorption frequency because the hydrogen bond strength decreases (Freund, 1974, Nakamoto et al., 1955).

In beryl and cordierite, examples of both positive and negative peak shifts were found. The positive shifts occur in minor, unidentified peaks, bending modes, or in rotational-vibrational combination bands. The shifts in the combination bands are caused by thermal excitation of low energy bands to successively higher states (Wood and Nassau, 1967). The type II H_2O asymmetric stretching bands in both cordierite and beryl show no peak shift. However, two other indexed H_2O stretching absorptions show substantial negative shifts, as does a lattice overtone at 1870 cm^{-1} (Fig. 3). In all three the rate of shift with temperature increases with temperature.

Figure 4 shows the behavior of the CO_2 which also occurs in the channels as cordierite. Because the CO_2 is not

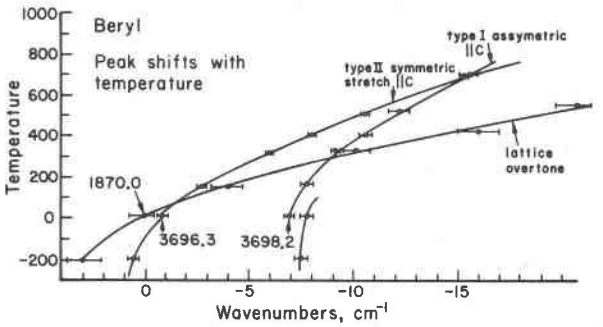

Fig. 3. Peak shifts for 3 absorptions in beryl, same sample used in Aines and Rossman, 1984b. The wavenumber scale is arbitrary and shows the relative shift of the peak position away from the 25°C value (which is shown on the graph). The curve for the type I assymetric stretching vibration (3698.2 cm^{-1}) has been shifted for clarity. The offsets in the two water curves at 25°C are apparently due to the fact that the −196°C spectra were run after the sample had been heated to 750°C, oxidizing some of the iron in it. Error bars are 95% limits based on estimated error in peak measurement. Curves have been drawn to fit the data smoothly.

bonded to the cordierite lattice, it is not expected to show a stretching vibration peak shift. No shift is seen in the central peak due to the asymmetric stretch. However, the side bands which appear to be rotational (or librational) combination modes shift toward each other and the stretching fundamental, with temperature. Apparently the frequency of the librational mode decreases with temperature, possibly due to expansion or rotation of the channel rings allowing slightly more free "rocking" of the CO_2 molecule. This has no effect on the stretching frequency, however.

Quartz

Upon heating quartz undergoes numerous changes in its O–H vibrational spectrum involving the interconversion of numerous OH defects which occur in a charge-compensating role for aluminum and alkali substitutions (Kats, 1962). The effect of heating on a natural hydrothermal quartz crystal containing only OH^- groups and no molecular H_2O is shown in Figure 5. The major changes result from a net dehydration of the crystal. The most stable defects are Al(OH) defects, which result in the three most intense peaks in the top spectrum of Figure 5 (Kats, 1962).

In situ high temperature spectra of this sample show that thermal broadening of peaks is an important effect on the spectroscopy of OH defects in quartz (Fig. 6). At −196°C 22 absorptions may be identified (this is typical in natural quartz; see Kats, 1962). At 577°C the spectrum has merged into a nearly featureless continuum, making it difficult to differentiate reactions among the O–H defect species. Accordingly we were unable to directly observe the changes documented in Figure 5.

Little change occurs over the range of the α–β transition (Fig. 6). The temperatures in this experiment are known to within ±1/2°C. The low gradients in this apparatus make us confident that the data in Figure 6 actually represent the α and β phases without temperature gradients causing par-

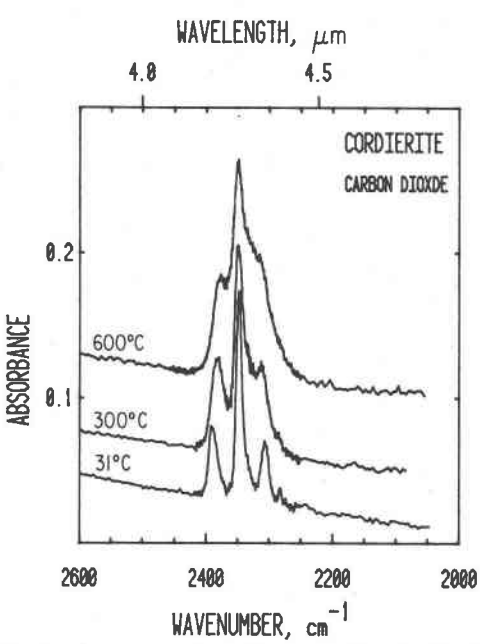

Fig. 4. Cordierite CO_2 absorptions. β and γ polarizations are mixed by a twin in the sample, however, the predominant direction is β. See Aines and Rossman, 1984b. Sample 16 μm thick. (Under perfectly polarized conditions, the central stretching mode is polarized in γ and the rotational-combination modes in β.)

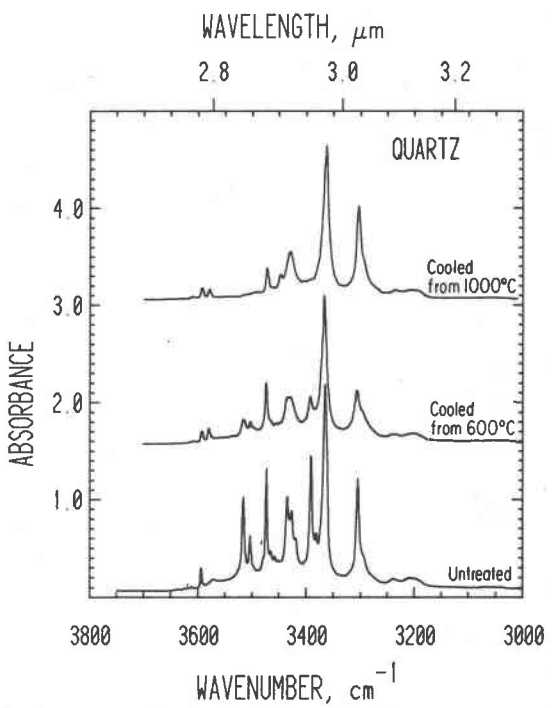

Fig. 5. Natural, flawless quartz crystal from Hot Springs, Arkansas. 5.07 mm thick, polarized E⊥*c*. Spectra obtained at −196°C after cooling from indicated temperatures.

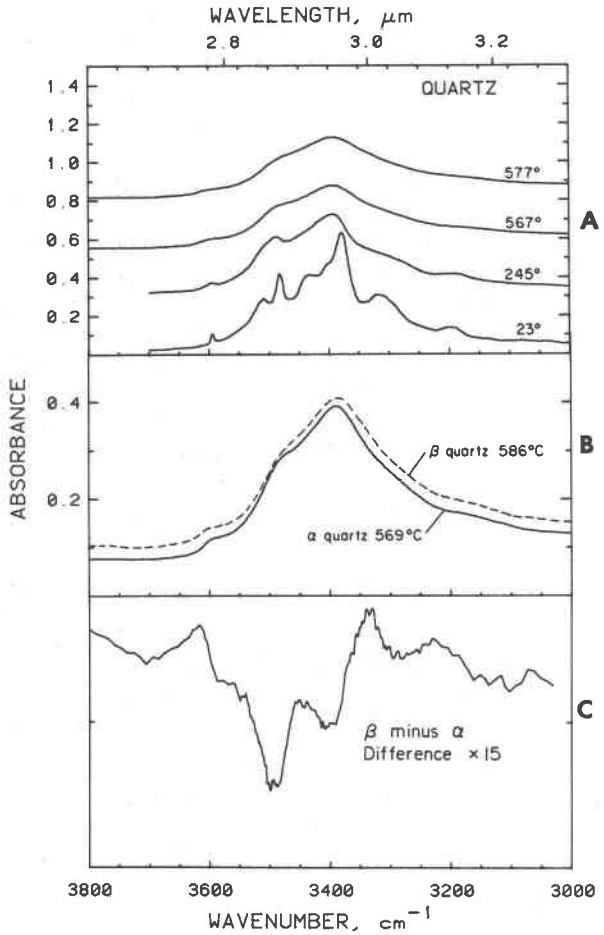

Fig. 6. Spectra of the same sample as Fig. 5, taken at temperature during the cycle up to 600°, through the α–β transition of 573°C (A) Polarized E⊥c. Spectrum after cooling is shown in Fig. 5, center trace. (B) Comparison of α and β quartz. (C) Difference between β and α spectra shown above, expanded vertically 15 times.

tial conversion. The changes seen in Figure 6B are reversible. The β minus α difference is seen in Figure 6C, expanded 15 times. These differences are very small, and it is not clear that they are a function of the phase change. The major areas where intensity is lost, 3400 and 3500 cm^{-1}, correspond roughly to the major peaks in the 23°C spectrum (Fig. 6) shifted to lower frequency by temperature. These peaks are due to Al(H) and Li(H) defects, respectively (Kats, 1962; Aines and Rossman, 1984a). Careful profiling in 2°C increments through the α–β transition showed that these changes are continuous over a 20° range, and are similar to changes occurring the same temperature range below the transition point. However, the α–β transition is also known to occur over a temperature range of 10° to 15°C (Van Goethem et al., 1977; Wright and Lehmann, 1981), consisting of a continuous increase in the effective area actually consisting of β quartz. From this we might expect changes in the IR spectrum to also occur over this range. Using a Mettler TA 2000 differential scanning calorimeter we have determined that the α–β transition in this sample occurs over a range of 570 to 575°C when heating at 0.2°/minute. The peak in the transition is at 573.5°C. Dolino et al. (1983) review the current literature on the α–β transition, and present high temperature IR spectra in the far-infrared which show a low frequency mode associated with the transition.

Metamict zircon

Metamict zircons from Ceylon contain a hydrous component, whereas zircons from the same locality that are not metamict are anhydrous (Woodhead, Rossman, and Silver, in preparation). The hydrous component in the metamict samples causes a broad, asymmetric absorption in the infrared and has been interpreted as hydroxyl groups in charge-balancing roles in the disrupted lattice, for instance H_2O forming SiOH and ZrOH groups from a broken Si–O–Zr bond (Aines and Rossman, 1985). Dehydration occurs more or less continuously above 400°C, but is rapid above 600°C. The more rapid loss of the low-frequency side of the band (Fig. 7) indicates that hydroxyl groups involved in short hydrogen bonds are being lost preferentially. Recrystallization occurs above 800°C, after most of the hydrous component is gone, suggesting that the hydroxyl groups stabilize the metamict state, and must re-form water before the bonds in the zircon lattice can re-form. The loss of the low-frequency component of the broad band at low temperatures indicates that the hydroxyl groups are involved in short hydrogen bonds, and hence high energy bonds, are expelled first.

It has been noted in broad bands in glasses that there is a reversible change in the band shape with temperature. The band shifts to higher energies, and loses integral intensity, both completely reversible and not associated with dehydration (Wedding, 1975). However, there is no difference in the zircon spectrum from 33° to −196°, while in hydrous glasses there is a pronounced increase in the low-frequency area of the band over this temperature interval.

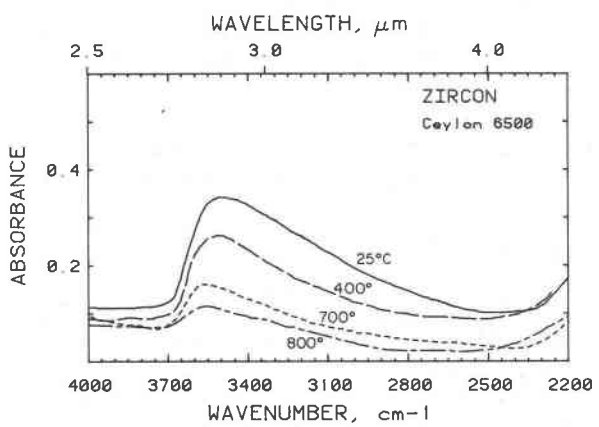

Fig. 7. Metamict zircon from Ceylon, sample #6500 from Aines and Rossman, 1985. Sample 0.3 mm thick, spectra are unpolarized.

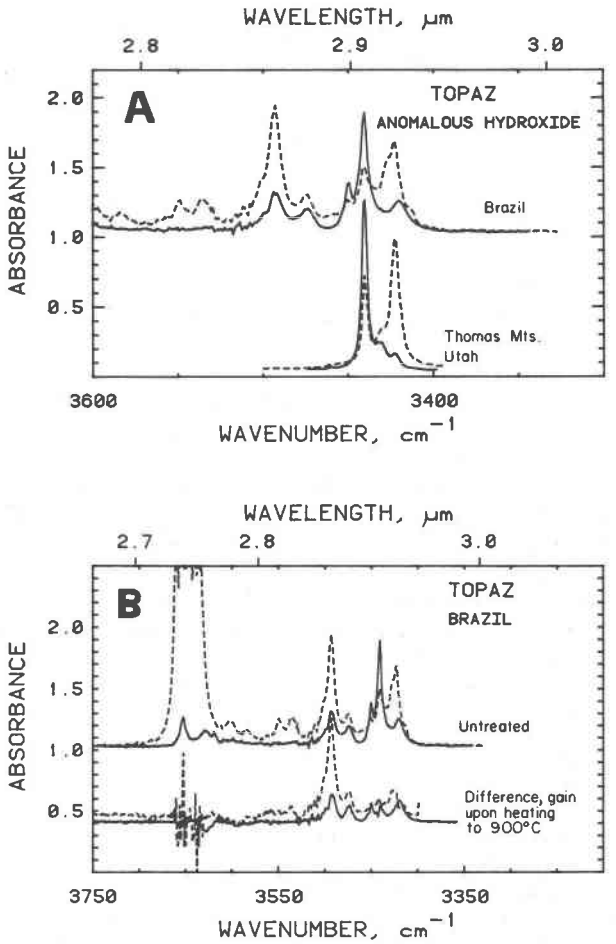

Fig. 8. OH absorptions in topaz caused by hydroxyl groups not in the crystallographically defined (OH^-, F^-) site. (A) −196°C spectra comparing colorless topaz from Minas Gerais, Brazil, to light brown topaz from the Thomas Mountains, Utah. The Brazilian sample is probably from a granitic pegmatite, typical of the region; thickness 0.6 mm. The Thomas Mts. topaz occur in vugs in rhyolite tuff; thickness 1.37 mm. The primary OH absorption at 3650 cm^{-1} is not shown. (B) Comparison of the Brazilian sample in (A) before heating, and the difference (untreated minus heated) showing absorptions lost after heating. No change occurred in the 3650 cm^{-1} primary absorption. Both A and B: dotted trace, α polarized; solid trace, β polarized.

The changes in shape in the zircon broad band are not reversible, indicating that there is a permanent change in the O–H–O distribution.

Topaz

Topaz ideally contains one (OH^-, F^-) site (Ribbe and Gibbs, 1971) which should result in a single OH stretching absorption in the infrared. However, topaz frequently shows numerous absorptions in the 4000 to 3000 cm^{-1} region. Many of these are sum and difference modes centering on the fundamental OH stretch at 3650 cm^{-1} resulting from the crystallographically identified "normal" hydroxyl site. At −196°C the difference bands related to this fundamental disappear (Aines and Rossman, 1985) and a number of "anomalous" secondary OH absorptions may be identified in the 3640 to 3200 cm^{-1} region (Fig. 8). These anomalous OH absorptions appear to be caused by hydroxyl groups; we have not observed a diagnostic H_2O band at 5200 cm^{-1} in the near-infrared region (Aines and Rossman, 1984a) in any topaz.

Neutron diffraction work by Parise et al. (1980) has revealed a second type of hydroxyl site in topaz. When two hydroxyl groups occupy adjacent (OH^-, F^-) sites, the protons approach too closely in the normal symmetry position, and instead are deflected to new positions. The original O–H vector lies between the α and γ directions, but when the protons are deflected to new sites the O–H vector will be in the αβ plane. This is the same polarization behavior observed for the anomalous peaks at ~3400 to 3450 cm^{-1}. However, there are numerous absorptions in that region, and Parise et al.'s lower symmetry site could only account for two absorptions. Also, there is no correlation between OH content and the intensity of the anomalous peaks. If paired hydroxyls were responsible they should increase with the OH/F ratio, but the anomalous absorptions are approximately the same in the Thomas Mountains samples which are fluorine-rich, and the Brazilian topaz which has much more hydroxide. Survey work of

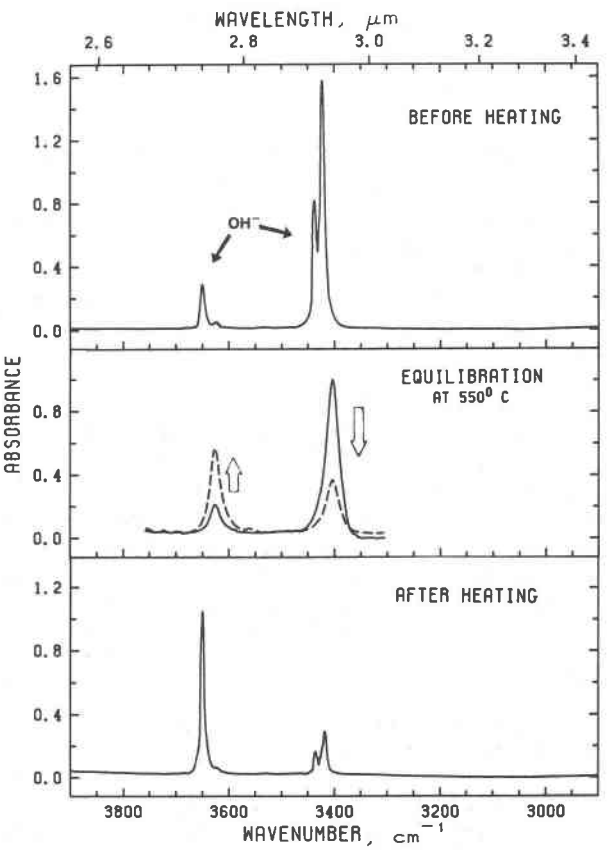

Fig. 9. Equilibration of hydroxyl sites in topaz from a rhyolite tuff, San Luis Potosi, Mexico. Sample 0.72 mm thick, polarized in the α direction. At 550°C, the anomalous hydroxide at 3400 cm^{-1} is seen converting to the normal hydroxide site.

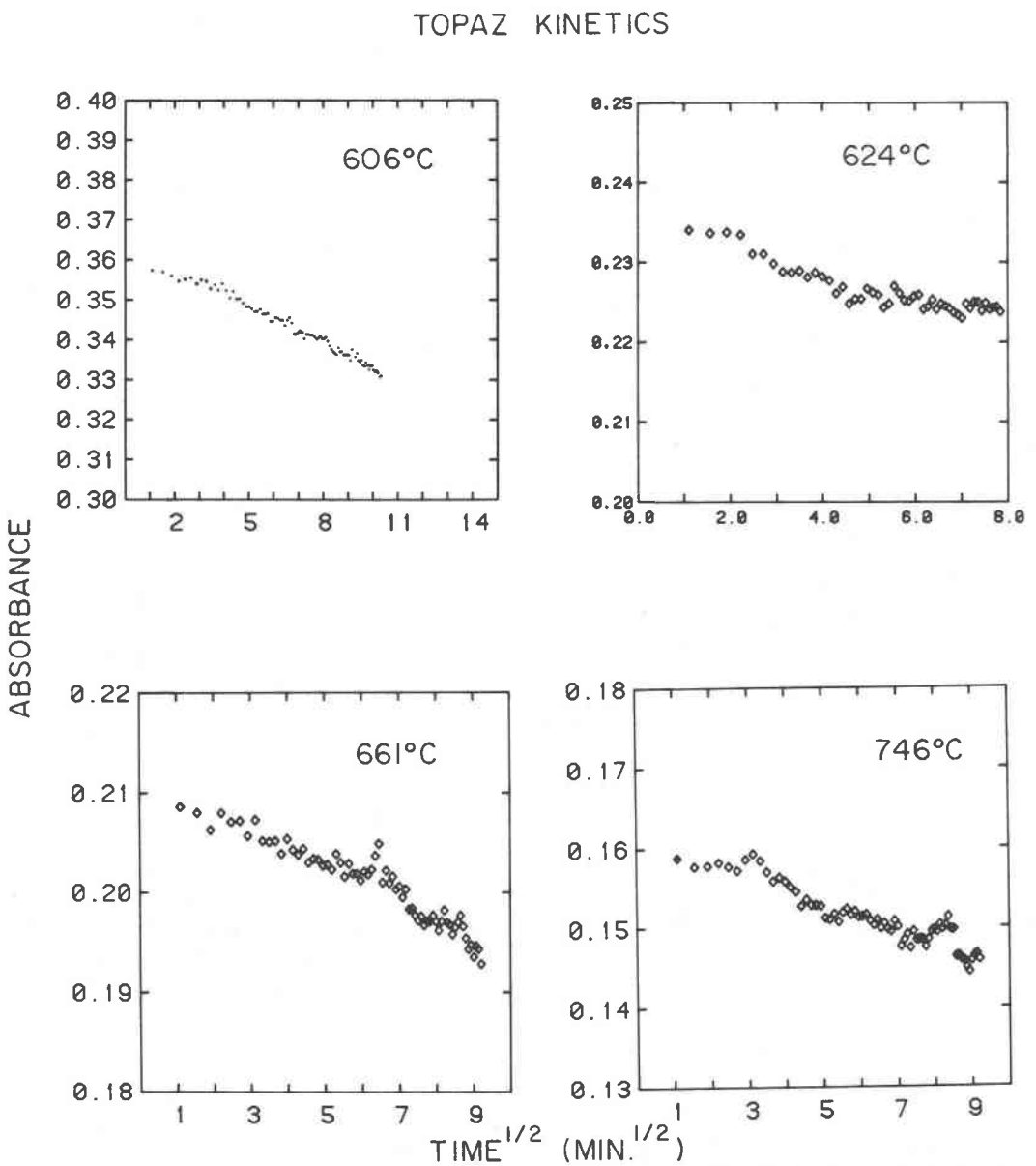

Fig. 10. Kinetics of the conversion shown in Figure 9. The absorbance of the anomalous hydroxide at 3400 cm^{-1} in α is plotted against (time)$^{1/2}$. The straight line relationships between absorbance, and hence concentration, and $t^{1/2}$ are consistent with a diffusional mechanism. Successive temperature plots are all from the same run; the reduction in rate is thus due to the reduction in available reacting species.

many topaz localities with OH/F ratios from ~0.02 to 0.5 shows no consistent variation in anomalous peak intensities which ranged from not detectable to the values seen in Figure 8.

Nevertheless, their thermal behavior is of interest. Aines and Rossman (1985) have shown that these absorptions are integrally related to radiation damage. Thermal treatment results in re-equilibration of hydrogen among sites. Figure 8B shows that in the Brazilian topaz, the peaks at 3450 to 3500 cm^{-1} disappear after heating to 900°C in air for 18 hours; no change was observed after 600°C. The peaks at 3400 to 3450 cm^{-1} showed little reduction in intensity. Topaz from rhyolites behaves differently, however. In these, there is a decrease in the 3440 cm^{-1} "anomalous" peaks concurrent with an increase in the "normal" peak at 3650 cm^{-1}. Figure 9 shows this change in topaz from San Luis Potosi, Mexico. In this sample, the dominant hydroxyl species is the one resulting in the 3440 cm^{-1} peaks, and the normal hydroxyl is subsidiary. Upon heating to above 400°C, however, the peaks can be observed changing intensity simultaneously (Fig. 9). The OH of the "anomalous" site is moving to the "normal" site. In Figure 10 the intensity of the 3400 cm^{-1} peak is plotted against (time)$^{1/2}$ at four temperatures run successively on the same sample.

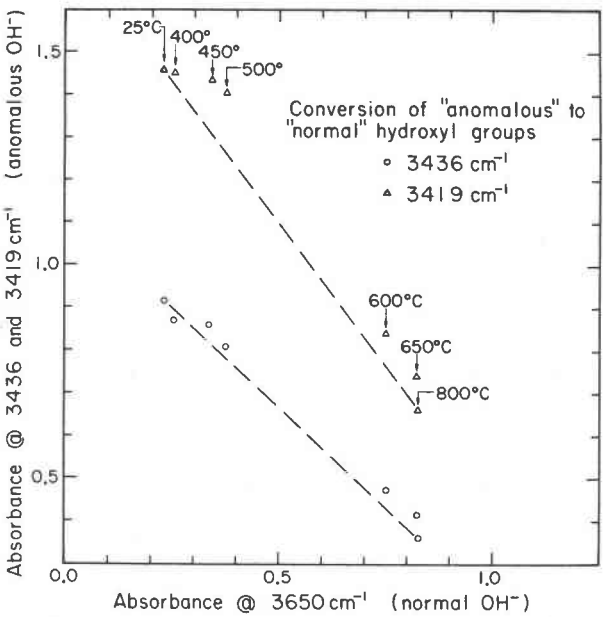

Fig. 11. Quantitative comparison of the peak heights of the two major anomalous OH peaks at 3436 and 3419 cm^{-1} in α, with peak height at 3650 cm^{-1} (normal hydroxyl) during a sequential heating experiment on topaz from the Thomas Mts., Utah. Sample 3 mm thick. Sample was held for 18 hours at the indicated temperatures, in air. Peak height measurements were then made at 25°C.

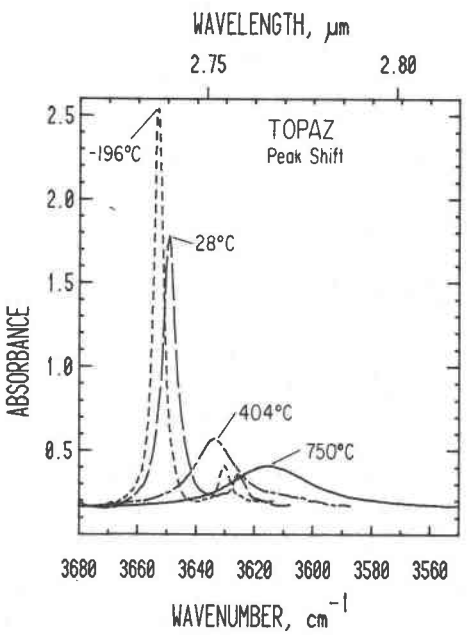

Fig. 12. Change in shape and position of the primary topaz OH absorption with temperature. Spectra from same experiment as Figure 11. Peaks have been scaled to reflect the peak intensity at 28°C after cooling from 750°C, since at each increasing temperature this peak grew in intensity. Polarized in α.

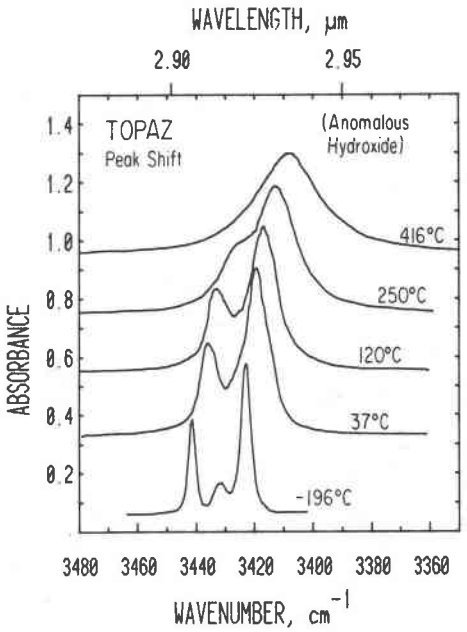

Fig. 13. Change in shape and position of the secondary OH absorptions with temperature. Same experiment as Figure 11. These spectra were obtained during the course of heating the sample from 37° to 416° over 15 minutes. No reaction occurred over this time. −196°C spectrum was run separately. Polarized in α.

The rate slows as the number of groups available to react becomes smaller at the higher temperatures. As such, an activation energy cannot be obtained from these data. However, the linear fits when plotted against $t^{1/2}$ are consistent with the interconversion mechanism rate-limiting step being diffusional in nature. Prolonged heating at 900°C did not result in complete conversion, however. About 10% of the original intensity at 3400 cm^{-1} remained.

This interconversion of hydroxyl groups was also investigated in a Thomas Mts. sample by stepwise sequential heating. The sample was held at temperature for 18 hours, then cooled, and the intensities at 3650, 3436, and 3419 cm^{-1} in α were measured. By making the measurement at 25°C we could measure the intensities of both the 3436 and 3419 cm^{-1} peaks which merge at high temperature (see Fig. 13). Contrary to the apparent result observed at high temperature, the interconversion of hydroxyl species does not quite occur in a 1:1 ratio (Fig. 11). The 3650 cm^{-1} peak gains intensity slightly more rapidly than the 3436 cm^{-1} loses intensity, as indicated by the lack of straight line behavior. (The slope of the line is related to the relative molar absorptivities which are not known, but appear to be similar.) The 3619 cm^{-1} peak comes much closer to a 1:1 conversion into the 3650 cm^{-1} peak.

This experiment suggests that there is an additional unidentified thermally unstable hydrous component in the topaz which also converts into the hydroxyl responsible for the 3650 cm^{-1} peak. It is not a major species, judging by

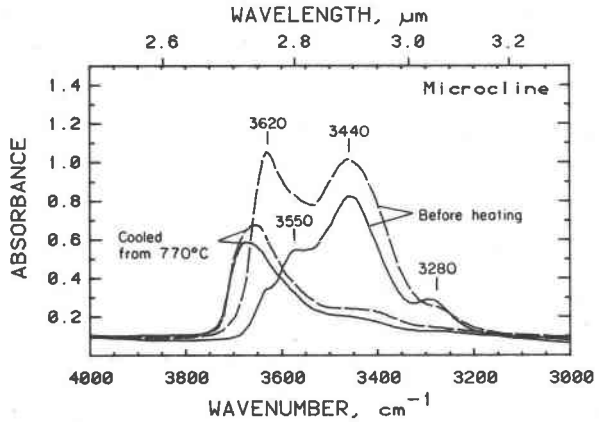

Fig. 14. Comparison of the before and after heating spectra of microcline showing the loss of both water types and the formation of a new, unidentified hydrous species. Spectra obtained at 25°C. Dash = α; solid = γ. Sample 0.38 mm thick, gemmy microcline (no fluid inclusions or turbidity) from the White Queen Mine, Pala, CA.

the minor deviation in Figure 11; however, we have not observed any additional absorptions in the rhyolite topazes which behave in this way.

The primary ("normal") OH absorption in topaz shifts 40 cm^{-1} lower in energy from $-196°$ to 750°C. The increase in half-width is also large, from 5 cm^{-1} to 30 cm^{-1} (Fig. 12). Although this change is dramatic because of the initial sharpness of the single peak, it is a similar increase to those seen in the other minerals in terms of total increase in width. The anomalous hydroxide peaks show similar broadening (Fig. 13) preventing resolution of the individual peaks above 400°C.

Feldspar

In collaboration with G. C. Solomon we have studied the changes in trace water speciation in microcline with temperature. Solomon and Rossman (in preparation) identify two types of molecular water in microcline (Fig. 14). Type I absorbs at 3620 and 3550 cm^{-1}, and type II at 3440 and 3280 cm^{-1}. Both are due to molecular water, identified by the 5200 cm^{-1} characteristic band.

Substantial changes occur in the spectra of water in microcline upon heating. Figures 15A and B show that the type II water is lost by 400°C. Solomon and Rossman have identified this water as occupying a very open site or defect, able to readily exchange. The rapid, low temperature loss confirms this. The type I water persists to 660°C. This water type has been identified by Solomon and Rossman as "structural," that is, occupying a well defined site in the feldspar structure. This water is necessary for the formation of amazonite (green) color in conjunction with lead and irradiation (Hofmeister and Rossman, 1985b).

Above 520°C a nearly isotropic band centered near 3690 cm^{-1} becomes apparent in both polarizations of the feldspar spectra. The spectra of Figure 15 do not conclusively demonstrate whether this is a new component, or whether the type I water peak at 3620 cm^{-1} simply shifts far enough to lower energy to expose the 3690 cm^{-1} band. The formation of this new band is irreversible. Comparison of the spectra of the sample cooled from 770°C to the original spectra (Fig. 14) clearly shows that a new hydrous

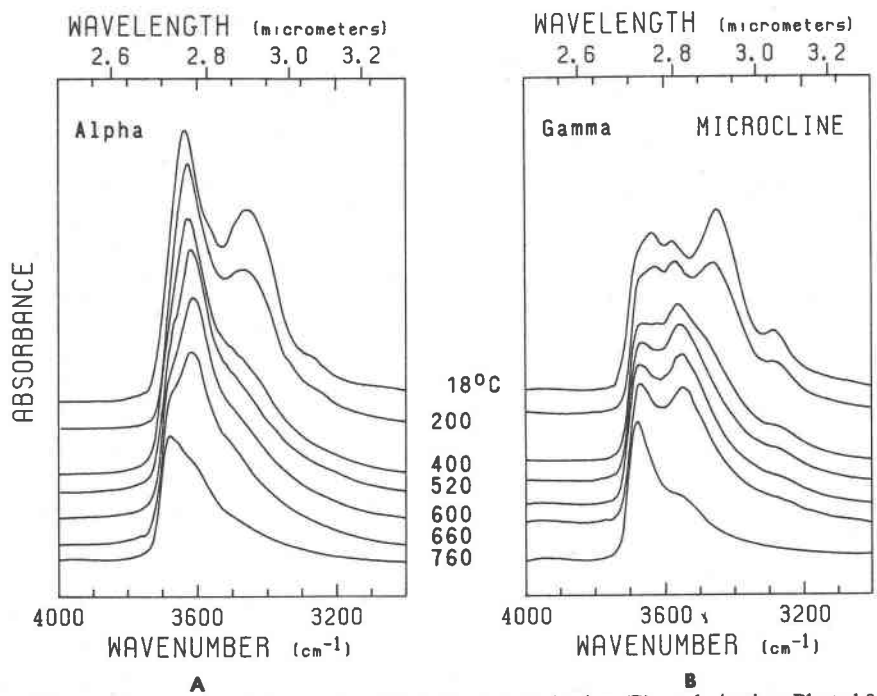

Fig. 15. High temperature spectra of the sample in Fig. 14. (A) α polarization, (B) γ polarization. Plotted 0.5 mm thick.

species has been created; the 3620 cm^{-1} peak could not have concealed the new peak. This is the only instance we have encountered of a major new species being formed irreversibly upon heating. The identity of this species is not known.

It seems unlikely that this feldspar originally crystallized at high temperature, or the type I water would not have been incorporated, instead reacting to form the new species seen here. However, both water types in the original sample may have formed during the slow transition to maximum microcline during cooling. Our experiment was not able to duplicate the slow cooling rate or water confinement that would be expected in a pegmatite, so we cannot verify this experimentally.

Lattice modes

During the course of high temperature observations of O–H absorptions, some information on the thermal behavior of lattice modes was also collected. In both quartz and muscovite lattice modes broaden and shift to lower frequencies with temperature (Fig. 16). In muscovite, the three bands that are on scale do not broaden greatly, while the off-scale absorption (near 1000 cm^{-1}) broadens considerably. In spectra taken during dehydration (at 750°C) this region was completely opaque, apparently due to structural changes in the mica.

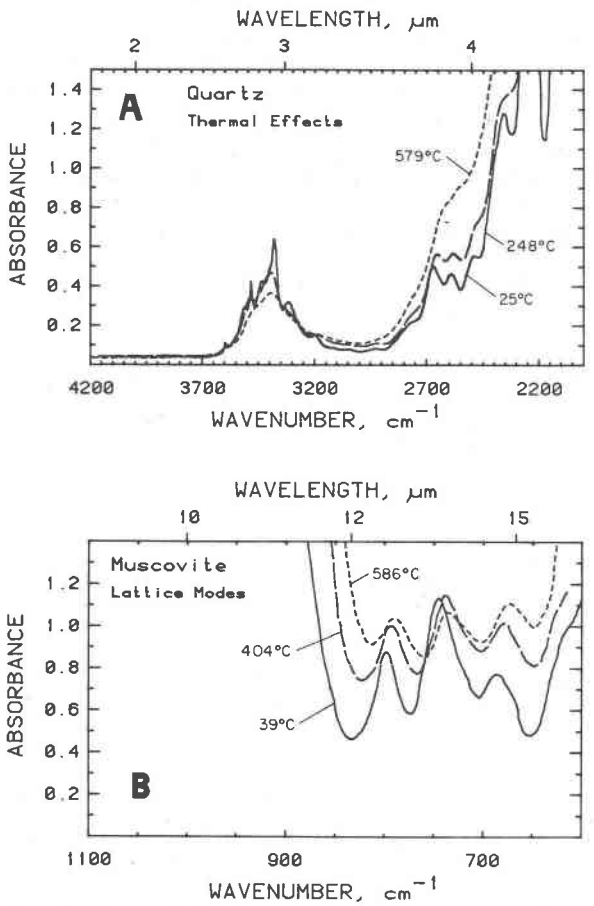

Fig. 16. Thermal effects on lattice infrared modes. (A) Quartz 5.07 mm thick, polarized E⊥*c*. Same samples as Figures 5 and 6. (B) muscovite, 11 μm thick, polarized in β. Same sample as Figure 2.

Conclusions

High temperature observation of water and hydroxide in minerals has revealed a wealth of reactions and behaviors. In muscovite and quartz, hydroxyl speciation appears much the same structurally at high temperature as at 25°C. In zircon, progressive dehydration and recrystallization occurs in metamict material. Cordierite and beryl both form an intermediate, gas-like H_2O species prior to dehydration (Aines and Rossman, 1984b). In topaz and feldspar, irreversible changes in hydrogen speciation are observed. There is suggestive evidence that a new, unidentified species forms in topaz as shown as a high-temperature intermediate between two hydroxyl species, but all other changes in speciation have been firmly identified as involving the oxygen–hydrogen species O–H and H_2O. For topaz, feldspar, beryl, and cordierite an understanding of the 25°C behavior of their trace hydrous components proves to be insufficient to understand that component at temperatures of geologic interest.

In all cases we have studied, O–H stretching absorptions in minerals show negative shifts with temperature. This indicates that hydrogen–bonding considerations are not controlling the peak shifts, since that should result in predominantly positive shifts. Integral IR intensities generally decrease slightly with temperature, as is expected as O–H–O distance increases, and the net dipole first derivative decreases. Broadening in all sharp O–H absorptions occurs to about the same extent (same number of $cm^{-1}/°C$), indicating that it is due to thermal motion of the hydrogen coordination environment rather than a fundamental quantum mechanical change in the hydrogen bonding with temperature.

Acknowledgments

We would like to thank G. Cleve Solomon (Caltech) for his help, collaboration, and discussion on the problem of water in feldspar. Jim Woodhead and L. T. Silver (Caltech) provided similar assistance with zircon. The zircon experiment was run by Chris Finch, and the quartz experiment by Martin Ruzek, while they were undergraduate research assistants. Their help is gratefully acknowledged. This work was supported in part by National Science Foundation grants EAR-79-19987 and EAR-83-13098.

References

Aines, R. D. (1984) Trace Hydrogen in Minerals. Ph. D. Thesis, California Institute of Technology, Pasadena, California.

Aines, R. D. and Rossman, G. R. (1984a) Water in minerals? A peak in the infrared. Journal of Geophysical Research, 89, 4059–4072.

Aines, R. D. and Rossman, G. R. (1984b) The high temperature behavior of water and carbon dioxide in the channels of cordierite and beryl. American Mineralogist, 69, 319–327.

Aines, R. D. and Rossman, G. R. (1985) Relationships between

radiation damage and trace water in zircon, quartz, and topaz. American Mineralogist, in press.

Aronson, J. R., Bellotti, L. H., Eckroad, S. W., Emslie, A. G., McConnel, R. K., and von Thüng, P. C. (1970) Infrared spectra and radiative thermal conductivity of minerals at high temperatures. Journal of Geophysical Research, 75, 3443–3456.

Dolino, G., Bachheimer, J., Gervais, F., and Wright, A. F. (1983) La transition α–β du quartz: le pont sur quelques problemes actuels: transition ordre-désordre ou displacive, comportment thermodynamique. Bulletin de Minéralogie, 106, 267–285.

Freund, F. (1970) Infrared spectra of $Mg(OH)_2$ at elevated temperatures. Spectrochemica Acta, 26A, 195–205.

Freund, F. (1974) Ceramics and thermal transformations of minerals. In V. C. Farmer, Ed., The Infrared Spectra of Minerals, p. 465–482. Mineralogical Society of London.

Hobbs, B. E. (1981) The influence of metamorphic environment upon the deformation of minerals. Tectonophysics, 78, 335–383.

Hofmeister, A. M. and Rossman, G. R. (1985a) A model for the irradiative coloration of smoky feldspar and the inhibiting influence of water. Physics and Chemistry of minerals, in press.

Hofmeister, A. M. and Rossman, G. R. (1985b) A spectroscopic study of irradiation coloring of amazonite: structurally hydrous Pb-bearing feldspar. American Mineralogist, in press.

Kats, A. (1962) Hydrogen in alpha-quartz. Philips Research Reports, 17, 133–195 and 201–279.

Kekulawala, K. R. S. S., Paterson, M. S., Boland, J. N. (1978) Hydrolytic weakening in quartz. Tectonophysics, 46, T1–T6.

Nakamoto, K., Margoshes, M., and Rundle, R. E. (1955) Stretching frequencies as a function of distances in hydrogen bonds. Journal of the American Chemical Society, 77, 6480–6486.

Parise, J. B., Cuff, C., and Moore, F. H. (1980) A neutron diffraction study of topaz; evidence for lower symmetry. Mineralogical Magazine, 43, 943–944.

Ribbe, P. H. and Gibbs, G. V. (1971) The crystal structure of topaz and its relation to physical properties. American Mineralogist, 56, 24–30.

Shankland, T. J., Nitsan, V., and Duba, A. G. (1979) Optical absorption and radiative heat transport in olivine at high temperature. Journal of Geophysical Research, 84, 1603–1610.

Stein, J. and Shankland, T. J. (1981) Radiative thermal conductivity in obsidian and estimates of heat transfer in magma bodies. Journal of Geophysical Research, 86, 3684–3688.

Van Goethem, L., Van Landuyt, J., Amelinckx, S. (1971) The α–β transition in amethyst quartz as studied by electron microscopy and diffraction. Physica Status Solidii (a), 41, 129–137.

Wedding, B. (1975) Measurements of high temperature absorption coefficients of glasses. Journal of the American Ceramic Society, 58, 102–105.

Wood, D. L. and Nassau, K. (1967) Infrared spectra of foreign molecules in beryl. Journal of Chemical Physics, 47, 2220–2228.

Wright, A. F. and Lehmann, M. S. (1981) The structure of quartz at 25 and 590°C determined by neutron diffraction. Journal of Solid State Chemistry, 36, 371–380.

Manuscript received, January 22, 1985;
accepted for publication, June 19, 1985.